OPTIMIZATION OF RADIAL EXTRUSION AND PELLET COATING PROCESSES USING PAT APPROACHES

A. Gradišek , G. Ratek , F. Vrečer , K. Korasa

PII: S0928-0987(23)00225-7
DOI: https://doi.org/10.1016/j.ejps.2023.106595
Reference: PHASCI 106595

To appear in: *European Journal of Pharmaceutical Sciences*

Received date: 29 May 2023
Revised date: 24 August 2023
Accepted date: 24 September 2023

Please cite this article as: A. Gradišek , G. Ratek , F. Vrečer , K. Korasa , OPTIMIZATION OF RADIAL EXTRUSION AND PELLET COATING PROCESSES USING PAT APPROACHES, *European Journal of Pharmaceutical Sciences* (2023), doi: https://doi.org/10.1016/j.ejps.2023.106595

OPTIMIZATION OF RADIAL EXTRUSION AND PELLET COATING PROCESSES USING PAT APPROACHES

A. Gradišek[1], G. Ratek[1], F. Vrečer[1,2], K. Korasa[1,*]

[1]Krka d. d., Novo mesto, Slovenia

[2]University of Ljubljana, Faculty of Pharmacy, Ljubljana, Slovenia

* Corresponding author:

- Phone: +386 7 331 3024
- E-mail: klemen.korasa@krka.biz

ABSTRACT

FDA's initiative Pharmaceutical CGMPs for the 21st century opened the door for introduction of several risk based approaches in pharmaceutical industry. One significant advancement that has emerged is the implementation of process analytical technology (PAT), which has opened doors for understanding and controlling complex technological processes. Two such processes, radial extrusion and pellet coating, offer a solid foundation for the application of PAT tools due to their numerous critical process parameters. The aim of the first part of the study was to optimize the neutral pellet production to produce the pellets with properties desired for successful film coating using design of experiments (DoE). In the second part the optimized pellets underwent film coating and the coating quantity was predicted in real or near real-time using in-line and at-line NIR probes and the performance of both probes was compared.

The desired properties of the pellets, narrow particle size distribution, high sphericity and high process yield, were successfully achieved. Models for film coating quantity prediction using in-line and at-line NIR probe were successfully calibrated and tested by coating two additional batches. Despite the limited sample size for model calibration, at-line NIR exhibited excellent prediction performance and enabled accurate determination of process end-point. The coating

quantity determined by UV/VIS spectroscopy in both test batches deviated by less than 2.0% from the target value. However, the in-line NIR probe, primarily due to its inferior spectral resolution, displayed a slightly lower quality of the calibrated model and notable overprediction for the tested batches.

Keywords: process analytical technology, radial extrusion, design of experiment, pellets, NIR, partial least squares regression

INTRODUCTION

In 2002, FDA announced a new initiative to implement risk-based modern approaches in pharmaceutical development, manufacturing and quality assurance to enhance and modernize the regulation of pharmaceutical manufacturing and product quality. Main objectives of the initiative were to encourage the early adoption of new technologycal advances, to facilitate the application of modern quality management techniques and to encourage the implementation of risk-based approaches (FDA, 2004a). One of the key technological approaches within this initiative is process analytical technology (PAT). FDA describes PAT as a system for designing, analyzing and controlling manufacturing through timely measurements of critical quality and performance attributes of raw and in-process materials and processes, with the goal of ensuring final product quality. Initiative categorizes PAT tools in four groups: Multivariate tools for design, data acquisition and analysis, Process analysers, Process control tools and Continuous improvement and knowledge management tools (FDA, 2004b). Multivariate tools for design, data acquisition and analysis include design of experiment (DoE) which is a multi-purpose technique of planning, designing and analysing the experiment so that valid and objective conclusions can be drawn (Antony, 2003). It is an efficient technique from the cost and work perspective, providing reliable results based on a relatively small number of experiments. Application of every DoE consists of selecting relevant measures of the system effectiveness or responses, independend variables to be varied, named factors and the levels on which selected factors are investigated (Barad, 2014). Designs can be divided to screening designs used in early stages of development, factorial designs and response surface designs, that are used in late stages for the optimization of process parameters. (Jankovic, 2021). To improve the efficiency and reduce the experimental bias of experimental design three principles, randomization, replication and blocking are used (Antony, 2003).

Extrusion, often paired with spheronization, is one of the most established methods of pellet manufacturing due to several advantages such as high process yield, narrow particle size distribution and low friability. Pellets produced by extrusion and spheronization method are therefore well suited for film coating. Process of extrusion and spheronization can be divided in several pharmaceutical operations or stages: granulation, extrusion, spheronization and drying (Aulton, 2018). In the first step granulation of powder blend with the granulation liquid is performed to obtain the plastic mass. Second step, extrusion, is the process of shaping the plastic mass into long rods. Extruders can be divided in four main classes: screw, sieve and basket, roll and ram. Further they can be divided into axial extruders, where the extrusion screen is positioned at the end of the axis of screw or rotor and radial extruders, where the extrusion screen is positioned around the axis (Vervaet, 1995). The third step of the process, i.e., spheronization, was not applied in the present study and the extrudates were dried in the fluid bed dryer immediately after the extrusion. Extrusion is a complex manufacturing process that depends on many process and formulation parameters (Ghebre-Sellassie and Knoch, 2007). Type and quantity of granulation liquid are both important formulation parameters that affect the plasticity of powder mass and its ability to be shaped into rods (Vervaet, 1994). Type of extruder can influence the size distribution, sphericity and density of pellets. Extrusion screen diameter of perforations determines the size of the pellets and the thickness of extrusion screen influences their density (Gandhi, 1999). Due to process cost optimization the extrusion speed in pharmaceutical production should be kept as high as possible. However, at higher speed surface impairments of extrudates such as roughness and sharkskinning can occur and lead to lower quality of the pellets (Vervaet, 1995). Large number of process and formulation parameters can be a reason for numerous difficulties in process optimization stage. Therefore use of advanced statistical methods such as DoE can significantly improve the success of process optimization. Several authors have used DoE in studies of extrusion. Désiré et al. (2011) used the response surface design to study the influence of water quantity, extrusion speed and extruder type in production of pellets containing active substance and microcrystalline cellulose. In another study Désiré et al. (2013) used a response surface design to investigate the quality of pellets produced with axial or radial extruder on laboratory and production scale. Loka et al. (2018) optimized the process and formulation parameters of pellets without MCC using five-factor, two-level fractional factorial design. Ibrahim et al. (2018) used two-factor, three-level full factorial design to optimize the formulation of theophylline pellets produced by screw extrusion and spheronization. Mallipeddi et al. (2013) used five-factor, two-level fractional factorial screening design to indentify the effects of formulation and process

parameters of extrusion and spheronization of pellets containing ethylcellulose, polyethylene oxide, microcrystalline cellulose and caffeine. Fractional factorial design was later expanded to produce a central composite design for response optimization.

Another commonly used approach in the group of Multivariate tools is partial least sqares regression (PLS), that is a method for constructing predictive models (FDA, 2004b), (Tobias, 1996). It is a statistical technique that allows comparison between multiple dependent response variables or Y and multiple independent explanatory variables or X. PLS allows the identification of underlying factors, that are a linear combination of independent variables which best model the dependent variables (Pirouz, 2006). Process analyzers are a branch of PAT tools, that provide large volumes of data by preferably non-destructive measurments of critical process and material attributes. They can be further divided into three groups: at-line where the sample is removed from the process stream and the analysis takes place in vicinity of the manufacturing site, on-line where the sample is once again removed from the process stream but can be returned after the measurement and in-line analysers that enable the measurments directly in the process stream in real-time (Korasa and Vrečer, 2018). NIR spectroscopy is one of the most promising and widely used process analysers for real to near-real time process monitoring due to its non-invasive and non-destructive measurement and no sample preparation required (Jamrógiewicz, 2012). NIR spectroscopy has two major disadvantages, being the requirement of calibration prior to process monitoring and its sensitivity to moisture content. (Korasa and Vrečer, 2018).

Simultaneous use of inter-connected PAT tools is necessary to enable their full potential for application in pharmaceutical industry (Korasa and Vrečer, 2018). Several authors used NIR spectroscopy for monitoring and predicting the coating thickness and sprayed quantity in the film coating process of pellets. Anderson et. al (2000) conducted in-line measurements using NIR probe inside a fluidized bed during film coating of pellets and calibrated a model with good predictability. Bogomolov et. al (2010) used the combination of Lighthouse NIR and Raman in-line probe for prediction of film-coating thickness and quantity of sprayed film-coating. Lee et. al (2011) calibrated an PLS model based on in-line NIR data and coating thickness measured using two different methods: confocal laser scanning microscopy (CLSM) image analysis and laser difraction particle size analysis, as a reference. Calibration models with good correlation ($R^2 > 0.995$) and ability to predict coating thickness were prepared. Marković et. al (2014) calibrated the models using consumption of coating solution and SEM coating thickness measurements as a reference on a production scale batches of pellets film-

coating. In-line and off-line NIR measurements were compared and slight superiority of off-line measurements in terms of accuracy and precision was shown. Hudovornik et. al (2015) evaluated the ability of coating thickness prediction with in-line NIR probe and in-line spatial filtering technique (SFT) size measurements.

Application of combination of PAT tools throughout all technological phases can improve the understanding of the pharmaceutical process and consequently improve the quality of final product. In the first part of the present study, the optimization of radial extrusion process by DoE was performed. The effect of process parameters water quantity, extrusion screen and extrusion speed was evaluated and the parameters were optimized to produce the microcrystalline cellulose based neutral pellets with narrow particle size distribution, high sphericity and high process yield. In the second part of the present study two commonly used PAT tools: NIR spectroscopy and PLS were combined to calibrate the model and predict the coating quantity during the pellet coating process. The aim of the study was to calibrate a PLS model for accurate film coating process end-point prediction and to compare the prediction performance of at-line and in-line NIR probe. Use of PAT tools for film coating process monitoring is beneficial, since it allows us direct and accurate determination of the film coating quantity in real time. Mentioned method has several advantages over monitoring the amount of sprayed material where several different factors such as flowmeter measurement variability, selective losses of coating dispersion, spray drying or variability in starting pellets size could cause the variability in applied coating quantity that can have significant effect on final critical quality attributes. To the best of authors' knowledge, there have been no published studies applying PAT tools to all steps of the production of film coated pellets, combining radial extrusion and film coating of pellets.

1. MATERIALS

Neutral pellets were manufactured using microcrystalline cellulose type 102 (MCC; Vivapur® 102; JRS Pharma, Germany) with average particle size 130 µm and binder polyvinyl-pyrrolidone (PVP; Kollidon® K-30; BASF; Germany). Suspension for film coating of pellets was prepared using polymer hydroxypropylmethyl-cellulose type 2910 with viscosity 6 mPas (HPMC; Pharmacoat® 606; Shin-Etsu; Japan), talc (Imerys talc; Italy) and tartrazine sodium salt (Sigma Aldrich, USA) that was used as a model active pharmaceutical ingredient based on its suitability for quantity determination using UV-VIS spectroscopy. Purified water was used as a solvent in granulation liquid and film coating suspension.

2. METHODS

2.1. Radial extrusion process

Mass for extrusion was prepared by high shear granulation (HSM; Gea UltimaGral™ 25; GEA; Germany) of 95 mg/unit MCC type 102 with granulation liquid consisting of 5 mg/unit PVP dissolved in purified water. Quantity of water was determined by experimental design presented in Table 1. Granulation liquid was sprayed using binary nozzle with diameter 1.2 mm (Schlick, Germany) with the speed of 120 g/min and atomization pressure of 1 bar. During the wetting phase, the impeller speed was set to 285 rpm and chopper speed to 1000 rpm. In the following 30 seconds long granulation phase the impeller speed was set to 400 rpm and chopper speed to 3000 rpm. The mass was extruded using (Gea NICA™ IPS25; GEA; Germany) radial extruder with dosing speed 40 rpm. Extrusion screen and extrusion speed were selected individually for each run according to the design as presented in Table 1. Extrudates were collected and dried in fluid bed dryer (GEA MP-1 S; GEA; Germany) to target product temperature 40 °C. Dried extrudates were milled using hammer mill (Frewitt Hammerwitt 3; Frewitt; Switzerland) with rotor orientation to blade side and speed 2500 rpm. Dosing speed was set to minimum 20 rpm and sieve size 1.0 mm was used to produce the final pellets.

2.2. DoE optimization of radial extrusion

The goal of experiments was to produce pellets with properties desirable for film coating using radial extrusion. Sphericity, width of particle size distribution of pellets and process yield were the measured responses being evaluated. Sphericity (SPHT) and width of particle size distribution were both determined using Camsizer XT image analyser (Retsch Technology, Germany). Width of particle size distribution was presented as parameter SPAN, calculated as the difference between 90th and 10th percentile of volume particle size distribution divided by median of volume particle size distribution as shown in Equation 1:

$$SPAN = \frac{d_{v,90} - d_{v,10}}{d_{v,50}} \qquad /1/$$

Sphericity of pellets was presented with the parameter SPHT that is calculated according to Equation 2, where P represents measured circumference of a particle projection and A represents measured area covered by a particle projection. For and ideal sphere SPHT is 1, otherwise it is smaller (Retsch Technology 2007).

$$SPHT = \frac{4\pi A}{P^2} \qquad /2/$$

Process yield was determined as a mass fraction of pellets after removing the dust fraction after milling process. Process and formulation parameters of radial extrusion were optimized using DoE. Factors used in DoE were quantity of water added to produce the granulation liquid, extrusion speed and extrusion screen, with the first two being the continuous numeric variables and the latter being the categorical variable on two levels. Design Expert® version 12 (Stat-Ease, Inc., USA) was used to design an optimal response surface design with 13 runs presented in Table 1. ANOVA was used to determine the influence of factors and their interactions on selected responses. Auto select function was used to perform the forward regression with criterion p-value and alpha 0.1 to select the significant model terms that were later included in ANOVA model. Hierarchy of the model was considered when selecting model terms. Numerical optimization with desirability function was used to find the best overall settings for the above-mentioned factors. Desirability function presented in Equation 3 is a geometric mean of the desirable ranges (d_i) for each response with desirable range zero being the least desirably and one the most desirable.

$$D = (d_1 \times d_2 \times \ldots \times d_n)^{\frac{1}{n}} = (\prod_{i=1}^{n} d_i)^{\frac{1}{n}} \quad /3/$$

2.3. Pellet coating

Several batches of pellets were produced at optimal process and formulation parameters determined using DoE and used in film coating experiments. The goal of these experiments was to calibrate and test a prediction model for pellet coating end point determination. Pellets were coated in bottom spray fluid bed coater (GEA MP-1 S; GEA; Germany) with 16.725% (w/w) water dispersion consisting of talc 8.3% (w/w), HPMC 8.3% (w/w) and tartrazine sodium salt 0.125% (w/w) to target weight gain of 20.15%. Final pellet composition is presented in Table 2. Calibration and testing batches were produced in the same batch size of 15.000 units, that corresponds to 1.5 kg of starting pellets. Wurster partition gap height was set to 2.0 cm and 1.2 mm binary nozzle (Schlick, Germany) was used to spray the coating dispersion at a rate of 20 g/min with atomizing pressure 1.5 bar. Inlet air flow rate was set to 120 m^3/h throughout the whole process and the inlet air temperature was varied between 65 and 70 °C to keep the product temperature in the target range of 35 to 40 °C. Inlet air humidity was set at 5.0 g/kg. Two NIR probes were used to monitor the process. In-line NIR probe Lighthouse probe® (GEA; Germany) was used to perform continuous measurements inside the pellet bed at a spectral range of 4750-9142 cm^{-1} with 10 second interval between individual measurements. Antaris Target analyser (ThermoFischer scientific, USA) at-line FT-NIR probe was used to measure

the spectra of samples, taken at predetermined points of the film coating process, at a spectral range of 5560-7400 cm^{-1}.

First two batches of film coated pellets were used as a reference to calibrate the model. Pellets were periodically sampled at predefined points calculated from coating suspension consumption ranging from 4% to 25% weight gain. For each sample time point of sampling was noted to find the corresponding in-line NIR measurement. Immediately after sampling at-line NIR spectra was measured. Samples were later analysed using UV/VIS spectroscopy to determine the tartrazine sodium salt content in coated pellets. Mass of pellets containing 0.2 mg to 0.3 mg of tartrazine sodium salt was weighed in headspace vials and dissolved in 20 mL of buffer with pH 6.8. Prior to measurement samples were filtered through 0.45 µm Millex syringe filters to remove the insoluble talc that could interfere with the UV-VIS measurements. Absorbance at wavelength 426 nm was measured using UV/VIS spectrometer. Quantity of tartrazine was calculated from absorbance data and used to calculate the quantity of film coating for each sample.

Unscrambler version 12.2 (Aspen Technology Inc.; USA) was used for data processing. Four consecutive measurements of each sample were taken by Antaris at-line NIR probe and the average was calculated. In the second step, standard normal variate (SNV) transformation was applied to normalize the spectra. Model was calibrated using partial least squares regression (PLS) using transformed spectral data in a range of 7407 cm^{-1} to 5557 cm^{-1} as an independent value or predictor (X). Quantity of film coating, calculated with the help of UV/VIS measurements, was used as a dependent value or response (Y). Kernel PLS algorithm was used for model calibration and full cross validation was performed. On the other hand, for in-line probe, more transformations of spectra had to be performed to produce a model of sufficient quality. In the first step Savitzky-Golay 1^{st} order derivative with 2^{nd} polynomial order and 5 smoothing points was performed. In the second step, spectra were normalized using SNV transformation. Model calibration was performed using PLS with the spectral data in a range of 8508 cm^{-1} to 6110 cm^{-1} as a predictor and quantity of film coating as a response. In the same way as for at-line probe Kernel PLS algorithm was used and a full cross validation was performed.

Ability to predict the film-coating quantity was tested on two film coating batches where pellets were sampled at random time points of the process. NIR spectra of taken samples were recorded and model prepared for at-line NIR probe was used to determine the coating quantity. Model was uploaded to Aspen Process Pulse version 12.2 (Aspen Technology Inc.; USA) to process

the NIR measurements and calculate the predicted values of film coating in real to near real-time. For at-line NIR probe time between sampling and acquisition of results was less than 1 minute and in-line NIR measurements were performed every 10 seconds. Process was stopped according to the goal to predict the process end-point at the target film coating quantity of 20.15 mg per unit using only NIR spectral data. In-line NIR spectra were also taken during the process, but were not used for end point prediction due to lesser model reliability. Samples taken during the test batches were also measured using UV/VIS spectroscopy to determine the actual film coating quantity through the contents of tartrazine. Determined quantities of film coating were compared to the values predicted with both prepared models.

3. RESULTS AND DISCUSSION

3.1. Radial extrusion optimization with DoE

In the first step of the research the goal was to optimize the selected process and formulation parameters of radial extrusion with the goal to produce pellets with properties suitable for film-coating in Wurster fluid-bed. A response surface design with two quantitative factors (quantity of granulation liquid and extrusion speed at three levels) and one categorical variable (extrusion screen size at two levels) was created and 13 experiments were performed with the goal to maximize the sphericity and process yield and minimize the width of particle size distribution.

Width of particle size distribution

Narrower width of particle size distribution of pellets ensures lower coating thickness variability among individual pellets after film coating and is therefore an important characteristic of pellets. Model terms water quantity ($p = 0.0064$), extrusion screen ($p < 0.0001$), interaction between water quantity and extrusion speed ($p = 0.0578$), squared term of water quantity ($p = 0.0064$) and squared term of extrusion speed ($p = 0.0408$) were found to have a significant effect on the width of particle size distribution. Although being insignificant, extrusion speed ($p = 0.2511$) was included in the reduced quadratic ANOVA model to keep its hierarchy. Model for width of particle size distribution proved to be significant ($p = 0.0001$) and individual points had a good fit ($R^2 = 0.9779$). Equation 4 presents the model with the factors where A stands for water quantity, B for extrusion speed and C for extrusion screen.

$$SPAN = 0.2971 - 0.0155A + 0.0048B - 0.0428C - 0.0113AB + 0.0244A^2 + 0.0162B^2 \quad /4/$$

Selection of extrusion screen had a significant effect on the width of particle size distribution. Larger extrusion screen 0.8 × 0.7 mm produced the pellets with narrower distribution as shown in Figure 1. Quantity of added water was another individual factor having a significant effect

but was also part of an interaction with the extrusion speed so they should be discussed together. Figure 2 shows the 3D response surface revealing that the SPAN value being the lowest in light blue coloured area which occurs at extrusion speed in the middle of the design space, at around 30 rpm and quantity of water in the upper half of the design space, at around 100 mg per unit. Interaction also shows that the value is at its highest point at low water quantities and high extrusion speed. That could tell us that extrusion of under wetted mass at high speeds produces extrudates of inadequate quality.

Sphericity

To ensure the homogeneity of film coating thickness throughout the whole pellet, starting pellets should be as round as possible. Factors Quantity of water, Extrusion screen and the interaction of both were proven to have a significant effect on the sphericity of pellets. Reducuced quadratic ANOVA model was created. Model with the coded factors where A stands for water quantity and C for the extrusion screen can be presented with Equation 5:

$$SPHT = 0.8497 - 0.0091A + 0.0344C + 0.0059AC - 0.0088A^2 \qquad /5/$$

Model above has proven to be significant ($p < 0.0001$) and individual points had a good fit ($R^2 = 0.9931$). Extrusion screen ($p < 0.0001$) and quantity of water ($p = 0.0085$) had a significant effect and were, due to their significant interaction discussed together. Figure 3 shows that use of 0.8 × 0.7 mm extrusion screen produces pellets with greater sphericity. It can be explained by extrudates produced with 0.8 × 0.7 mm being less elongated and can be more easily cut to even pieces during the milling process, compared to those produced with 0.5 × 0.5 mm screen. Effect of water quantity is more pronounced at smaller extrusion screen 0.5 × 0.5 mm and causes the sphericity of pellets to decrease with increasing water quantity, whereas the effect is less visible when using the larger extrusion screen. The effect of extrusion speed was not significant ($p = 0.4302$), therefore it was not included in the final model.

Process Yield

Process yield is an important factor in pharmaceutical processes and should therefore be as high as possible. In this study process yield was determined by weighing the pellets after sifting out the dust fraction after milling. Because pellets passed a sieve with mesh size 1.0 mm to exit the milling chamber no agglomerates were present and therefore additional sieving of agglomerates was not necessary. Quantity of water, extrusion screen and their interaction had the significant effect ($p < 0.0001$), therefore reduced 2FI ANOVA model was created using these three terms.

Model with the coded factors where A stands for water quantity and C for the extrusion screen can be presented with the Equation 6:

$$\text{Process Yield} = 89.42 + 3.60A - 7.79C + 3.96AC \qquad /6/$$

Model above proved to be significant ($p < 0.0001$) and individual points had a good fit ($R^2 = 0.9857$). Due to two individual factors and their interaction being terms of equation they should be discussed together. Figure 4 shows that using 0.5 × 0.5 mm screen process yield is much better and not significantly affected by water content, whereas with 0.8 × 0.7 mm screen process yield is lower but can be greatly improved by increasing the water quantity. Greater yield of 0.5 × 0.5 mm sieve usage can be contributed to the same 1.0 mm sieve used in the milling process and smaller milled particles could pass that sieve easier and faster, therefore being in the milling chamber for shorter time compared to larger particles produced by 0.8 × 0.7 mm extrusion screen. Due to shorter contact with the milling area smaller amount of dust fraction is produced and the process yield is higher. Additionally, higher yield could be a consequence of a higher density and therefore lower friability achieved with smaller extrusion screen size. Effect of higher water quantity on process yield can be explained by pellets being produced with higher water quantity being more resistant and less susceptible to being pulverized during the milling phase.

Process optimization

Based on models prepared for each of the monitored responses numerical optimization was performed. Goal of optimization was to maximize the sphericity and process yield and minimize the width of particle size distribution. All of the top six solutions of numerical optimization, presented in Table 3 had optimal quantity of water 110 mg per unit and extrusion screen 0.8 × 0.7 mm and same desirability (0.824) at all of the suggested extrusion speeds ranging between 35.874 rpm and 44.056 rpm. However, solution number one with extrusion speed 37.5 rpm was taken into further consideration due to experiment with the run order 12 being produced with the same parameters as the solution. The actual measured values of responses for run 12 were used in model confirmation step and were compared to the predicted values for these responses. Results of confirmation are presented in Table 4 and show that all considered values of experimental batch were inside the 95% confidence interval of prediction, therefore it was concluded that the proposed process parameters are suitable for further use. Optimized process of radial extrusion was used to manufacture pellets used in film-coating trials in the second part of the study.

3.2. Film coating model calibration

A PLS model for coating quantity prediction was calibrated for both NIR probes, based on differences in the intensity of NIR bands belonging to components of film coating. SNV transformed NIR spectra of the same sample are presented in Figure 5. Band of talc at wave number between 7180 cm^{-1} and 7160 cm^{-1} is the most distinct band where changes in film coating quantity can be observed and therefore contributes the most to spectral variability. Using at-line probe it appears as a narrow sharp band. With in-line probe the same band is shallower and broader, due to inferior resolution of the in-line probe in comparison with the at-line one. With at-line probe second, smaller band of talc at 7140 cm^{-1} was also detected and contributed a small portion to total variability. However, with in-line probe second band of talc was not detected due to lower resolution. Third distinct band belonging to film coating components was a shallow, broad band of HPMC at wave number between 5900 cm^{-1} and 5400 cm^{-1}. Absorption band of water at 6940 cm^{-1} (1440 nm) is in a close proximity to both bands of talc and could in theory affect the measurements. Second absorption band of water at 5180 cm^{-1} (1930 nm) was detected only by in-line probe and showed some differences among batches. Besides that, slight decrease of absorption band intensity during the coating process was observed and could be contributed to the decrease in the residual moisture content. At-line probe measures in spectral range up to 5557 cm^{-1} so the absorption band of water was not detected. Comparing NIR spectra from both probes it can be observed, that using at-line probe spectra with good resolution in a narrower spectral range are obtained. Meanwhile in-line probe measures in a wider spectral range and in real time, but has inferior resolution, that can reduce the sensitivity of the model.

<u>Calibration of model for Antaris at-line probe</u>

For calibration of model for at-line probe spectral data throughout the whole spectral range of the probe was taken. Average of four measurements of each sample was calculated and SNV transformation was carried out to prepare spectra for further processing. PLS model was calibrated using spectral data as predictors and film coating quantity calculated from the tartrazine assay as a response. Full cross validation was also performed with the same set of data.

Calibrated model had practically whole (99.64%) variability explained by the 1st factor. Therefore it was the only factor included into the final model. Figure 6 shows weighted regression coefficients plot where contribution to total model variability by each wave number of the spectra is displayed. Majority of variability occurs due to main band of talc at

approximately 7170 cm^{-1} and some smaller portion of variability is contributed by the smaller absorption band of talc next to the main one and band of HPMC between 5900 cm^{-1} and 5600 cm^{-1}. Analysing Predicted vs Reference plot shown in Figure 7, linearity of the model is observed throughout the complete experimental space. Linear calibration curve slope (0.9964) and offset (0.27%) show great correlation between the predicted and reference values. Inspecting individual points no outliers are visible which is confirmed by low root mean square error (RMSE) 1.95% and high R^2 0.9964. Validation slope (0.9942), offset (0.33%), RMSE (2.30%) and R^2 (0.9957) are similar to the calibration curve values. Individual validation points also show no visible deviations from calibration points. Therefore, reliable prediction in the test batches can be expected using the model for at-line probe.

Calibration of model for Lighthouse in-line probe

Calibration of model for in-line probe was performed with spectral data in the spectral range of 8508 cm^{-1} to 6110 cm^{-1}. To minimize unwanted spectral variability in the region around the absorption band of water (5180 cm^{-1}), spectral region from 6110 cm^{-1} to 4874 cm^{-1} was not taken into consideration for model calibration. Savitzky-Golay 1st derivative transformation with 2nd polynomial order and 5 smoothing points had to be performed to improve the spectral resolution and remove interferences of broader bands improving the focus on a narrower band of talc. Film coating quantity calculated from the tartrazine assay was taken as a response. Full cross validation was also performed with the same set of data used in calibration of the model.

Factor 1 of a calibration model explained a large portion of variability (98.21%). Therefore, it was decided to produce the final model with a single factor, same as for the at-line probe. In weighted regression coefficients plot shown in Figure 8, contribution of derived talc absorption band is visible at wavelength between 7220 cm^{-1} and 7150 cm^{-1}. Small negative contribution of water absorption band around 6940 cm^{-1} is also visible and is attributed to the water content in pellets getting slightly lower throughout the whole process. Due to proximity to the talc absorption bands effect of water content can possibly influence the prediction. Predicted vs Reference plot (Figure 9), shows a linear model throughout the complete experimental space. Linear calibration curve slope (0.9821) and offset (1.26%) show good correlation between the predicted and reference values. Deviation of individual points is slightly larger in comparison with the Predicted vs Reference graph for at-line probe which is also confirmed by larger RMSE (4.92%) and slightly lower R^2 0.9821. However, both values still point towards a very decent prediction model. Validation slope (0.9792), offset (1.32%), RMSE (5.71%) and R^2 (0.9789) are similar to the calibration curve values and individual validation points show no visible

deviations from calibration points. It can be concluded that even though the prediction model for the in-line probe is not as good as the one for the at-line probe still a decent prediction of film coating quantity can be expected.

3.3. Film coating model testing

Both models were tested by coating additional two batches and monitoring the predicted film-coating quantity in the real or near real-time. The goal of the experiments was to predict the target film coating quantity of 20.15 mg per unit and stop the process when that point was reached. Due to better reliability process was stopped according to the model for at-line probe, while the second model for in-line probe was used as a comparison. Several samples were taken during the process to be analysed using at-line NIR probe for coating quantity prediction and later the results were confirmed by UV/VIS determination of tartrazine assay. Results of coating quantity below are presented as the percentage of the target film coating quantity 20.15 mg per unit.

Results of film coating of the first test batch are presented in Table 5. Film coating quantity after measurement of sample 5 (98.5%) was close to the target value of 100%. Therefore film coating process was stopped shortly after the at-line NIR measurement of sample 5 was performed. Pellets were dried and another sample was taken after drying. Surprisingly high prediction of the at-line probe model (108.7%) was obtained. Film coating quantity of the sample after drying determined by tartrazine assay was 101.9% and pointed towards the overprediction of the model. Overprediction could be explained by the lower residual moisture that can increase the predicted value of film coating quantity as the overlapping of talc and water absorption bands can occur due to their proximity. Loss on drying (105 °C, 5 min, 2 g) for the dried sample of the first test batch was 1.89% and is considerably lower in comparison to the calibration batches with loss on drying 2.9-3.5%. Despite regression coefficient graph for at-line NIR probe (Figure 6) showing no visible contribution of water to the model variability the experiments show the effect of drying on the predicted value. It can be assumed that the removal of the residual moisture affected the relative intensity of the talc absorption bands and therefore exaggerated the prediction. Besides that some overprediction, on average 5%, was observed throughout the whole test batch and could be the consequence of the differences in residual moisture content among batches. Predicted vs. reference plot for at-line NIR model shows linear correlation of individual points with slope 1.010 and offset 3.77%. Positive offset and slope greater than 1 again point on model overestimation in all evaluated samples and that the overestimation is increased at higher coating quantities. Coefficient of determination (R^2)

for given model was 0.8456 and RMSEP was 4.88%. For in-line probe spectra were taken continuously and are presented in Figure 10. In the points where the samples were taken, predictions were compared to the actual values of film coating quantity determined by tartrazine content and are presented in Table 5. Throughout the whole process the predicted coating quantity is constantly higher without bigger deviations of individual points. By comparing predictions to actual values of taken samples it showed, that in-line probe overpredicted an actual value by 15% on average. Despite the notable overprediction of the at-line NIR probe model for the final dried sample the actual coating quantity (101.9%) was relatively close to the target value, therefore the experiment was successful for at-line probe. However, for in-line probe further improvements of the prediction model have to be made to produce a more accurate model.

Coating process was repeated using same process parameters. The results of second test batch are presented in Table 6. Film coating process was stopped after the model for at-line NIR probe predicted film coating quantity of 100.0% for sample number 6. Another sample (number 7) was taken immediately after spraying process termination and coating quantity of 100.5% was predicted. After drying the pellets, the model predicted film coating quantity of 104.9%. Increase in prediction after drying confirms the effect of residual moisture content on model overprediction, which occurs due to relative proximity of water and talc absorption bands. Analysing the actual quantity of film coating by tartrazine content showed 100.1% of the target value for the final dried sample. In comparison to the first batch fit between predicted and actual values was better. However, in this case, the model once again exhibited overprediction of the film coating quantity, averaging a 3% overestimate compared to the initial batch's average overprediction of 5%. Further analysing the predicted vs. reference plot for at-line NIR model good linear correlation with slope 1.027 and offset 0.70% was observed. Coefficient of determination (R^2) for given model was 0.9754 and RMSEP was 3.32%. Second batch showed excellent correlation of predicted values to the reference and was superior in comparison with the first one. Reason for different model performance between both batches could be in different residual moisture contents. Another possibility could be different rates of talc sedimentation batches and consequently difference in quantity delivered on pellets. Prediction based on spectra continuously taken using in-line probe are shown in Figure 11. Linear film coating quantity with no major deviations of individual measurements is observed throughout the whole process. Plotting the predictions of the model for the in-line probe overprediction is observed again, similar to first test batch. Difference between actual and predicted values is from 8% to

14% with an average of 11%. That is slightly better compared to the first batch and is consistent with the results for at-line NIR. However, the results confirm that further enhancements are required for the in-line probe model in order to improve its reliability.

One of the main reasons for relatively inaccurate prediction of the in-line probe model could be low resolution of the probe. Consequently the talc absorption band is relatively shallow and wide in comparison to the sharp one obtained by the at-line probe. On that account less spectral variability is achieved at minimal coating quantity differences and therefore the model is less accurate. On the other hand, despite 3-5% overprediction, the results obtained by the at-line probe model were satisfactory and the model shows great promise for accurate and reliable prediction with minimal improvements. Considering that the model was calibrated using only two batches, increasing the sample size for model calibration has the potential to greatly enhance both the accuracy and reliability of the model. Effect of residual moisture content on model prediction was observed testing the samples taken after drying of pellets. The observed effect is likely contributed to the overlapping of water and talc absorption bands, which occurs due to their close proximity. Inclusion of several reference batches prepared at different residual moisture contents during the process could also improve the robustness of the model and reduce the effect of the moisture content. With talc being suspended in coating dispersion a sedimentation and selective loss of talc can occur during the film-coating process. Possible differences in sedimentation rate among batches could lead to deviations in model prediction. Again preparing larger number of experiments for model calibration could minimize the risk of variability in quantity of talc actually delivered on pellets.

4. CONCLUSION

In the present study, DoE was applied successfully to optimize critical process parameters for production of pellets with properties favourable for film coating. The goal of the experiments was to produce pellets with high sphericity and narrow distribution of particle size with as high as possible process yield. Pellets with most desirable properties were produced by use of larger extrusion screen (0.8 × 0.7 mm) in combination with the water quantity in the upper limit of design space (110 mg per unit) and extrusion speed in the middle of design space (37.5 rpm). Study showed the value of DoE application in development and optimization of formulation and process in pharmaceutical industry.

The PLS model for coating quantity prediction was calibrated using NIR spectral data as an independent variable and coating quantity, calculated from UV/VIS determination of tartrazine

assay, as a dependent variable. Two different NIR probes were applied to monitor the film coating process. At-line probe showed good resolution and provided the spectra with distinct and sharp absorption bands. On the other hand, the spectra obtained by in-line probe had less distinct absorption bands, which made the calibration more difficult. Subsequently the prediction of film coating quantity with at-line probe was relatively good despite slight overprediction, up to 5%. Overprediction of the model, calibrated using the in-line probe data was considerably larger, up to 15%. Said results back the decision to use the at-line probe model as a reference to determine the film coating process end-point. Despite the overprediction of the at-line model both first and second batch were successfully finished in time to provide the pellets with 101.9% and 100.1% of target film coating quantity respectively. Effect of residual moisture due to proximity and possible overlapping of talc and water absorption bands was observed and can play a significant role in model overprediction. Since the models were calibrated using data from only two batches, expanding the sample size for model calibration has the potential to provide even greater improvements to the model. Experiments proved that the calibration of models was successful and that accurate film coating end point prediction with the at-line NIR probe is possible. Talc being a part of numerous film coating formulations offers a great basis for NIR detection and determination, due to its two sharp absorption bands between 7100 cm^{-1} and 7200 cm^{-1}. However, experiments showed that NIR probe with sufficient resolution has to be used to fully detect both absorption bands and provide the desired quality of spectra for model calibration and prediction of film coating quantity.

ACKNOWLEDGMENT

This research has been supported by Krka, d. d., Novo mesto.

REFERENCES

Andersson, M., Folestad, S., Gottfries, J., Johansson, M.O., Josefson, M., Wahlund, K.G. 2000. Quantitative analysis of film coating in a fluidized bed process by in-line NIR spectrometry and multivariate batch calibration. Anal. Chem. 72, 2099–2108. http://dx.doi.org/10.1021/ac990256r

Antony, J. Fundamentals of Design of Experiments. In: Antony J. Design of Experiments for Engineers and Scientists. Oxford: Butterworth-Heinemann; 2003. p. 6-16. https://doi.org/10.1016/B978-0-7506-4709-0.X5000-5

Aulton, M.E. Powders, granules and granulation. In: Aulton, M.E., Taylor, K.M.G. Aulton's Pharmaceutics The Design and Manufacture of Medicines. Fifth Edition. Elsevier; 2018. p. 476-497.

Barad, M. 2014. Design of Experiments (DOE)—A Valuable Multi-Purpose Methodology. Applied Mathematics, 5, 2110-2129. http://dx.doi.org/10.4236/am.2014.514206

Bogomolov, A., Engler, M., Melichar, M., Wigmore, A. 2010. In-line analysis of a fluid bed pellet coating process using a combination of near infrared and Raman spectroscopy. J. Chemom. 24, 544–557. http://dx.doi.org/10.1002/cem.1329

Désiré, A., Paillard, B., Bougaret, J., Baron, M., Couarraze, G., 2011. A Comparison of three extrusion systems - Part I: The influence of water content and extrusion speed on pellet properties. Pharmaceutical Technology, 35(1), 56–65. [WWW Document]. URL https://www.pharmtech.com/view/comparison-three-extrusion-systems (accessed 2.5.2023)

Désiré, A., Paillard, B., Bougaret, J., Baron, M., Couarraze, G., 2013. Extruder scale-up assessment in the process of extrusion–spheronization: comparison of radial and axial systems by a design of experiments approach, Drug Development and Industrial Pharmacy, 39:2, 176-185, https://doi.org/10.3109/03639045.2012.665458

FDA 2004a. Pharmaceutical CGMPs for the 21s Century - A risk-based approach. [WWW Document]. URL https://www.fda.gov/media/77391/download (accessed 26.4.2023)

FDA 2004b. Guidance for Industry PAT — A Framework for Innovative Pharmaceutical Development, Manufacturing, and Quality Assurance. [WWW Document]. URL www.fda.gov/media/71012/download (accessed 26.4.2023)

Gandhi, R., Lal Kaul, C., & Panchagnula, R. (1999). Extrusion and spheronization in the development of oral controlled-release dosage forms. Pharmaceutical Science & Technology Today, 2(4), 160–170. https://doi.org/10.1016/S1461-5347(99)00136-4

Ghebre-Sellassie, I., Knoch, A. Pelletization Techniques. In: Swarbrick, J. Encyclopedia of Pharmaceutical Technology. Third Edition. New York: Informa Healthcare; 2007. p. 2651-2663.

Hudovornik, G., Korasa, K., Vrečer, F., 2015. A study on the applicability of in-line measurements in the monitoring of the pellet coating process. Eur. J. Pharm. Sci. 75, 160–168. http://dx.doi.org/10.1016/j.ejps.2015.04.007

Ibrahim, M. A., Zayed, G. M., Alsharif, F. M., Abdelhafez, W. A. 2019. Utilizing mixer torque rheometer in the prediction of optimal wet massing parameters for pellet formulation by extrusion/spheronization. Saudi Pharmaceutical Journal, 27(2), 182–190. https://doi.org/https://doi.org/10.1016/j.jsps.2018.10.002

Jankovic, A., Chaudhary, G., Goia, F. 2021. Designing the design of experiments (DOE) – An investigation on the influence of different factorial designs on the characterization of complex systems. Energy and Buildings, 250, 111298. https://doi.org/https://doi.org/10.1016/j.enbuild.2021.111298

Jamrógiewicz, M. 2012. Application of the near-infrared spectroscopy in the pharmaceutical technology. J. Pharm. Biomed. Anal. 66, 1–10. http://dx.doi.org/10.1016/j.jpba.2012.03.009

Korasa, K., Vrečer, F. 2018. Overview of PAT process analysers applicable in monitoring of film coating unit operations for manufacturing of solid oral dosage forms. European Journal of Pharmaceutical Sciences, 111, 278–292. https://doi.org/10.1016/j.ejps.2017.10.010

Lee, M.J., Seo, D.Y., Lee, H.E., Wang, I.C., Kim, W.S., Jeong, M.Y., Choi, G.J. 2011. In line NIR quantification of film thickness on pharmaceutical pellets during a fluid bed coating process. Int. J. Pharm. 403, 66–72. http://dx.doi.org/10.1016/j.ijpharm.2010.10.022

Loka, N. C., Saripella, K. K., Pinto, C. A., Neau, S. H. 2018. Use of extrusion aids for successful production of Kollidon® CL-SF pellets by extrusion–spheronization. Drug Development and Industrial Pharmacy, 44(4), 632–642. https://doi.org/10.1080/03639045.2017.1405975

Marković, S., Poljanec, K., Kerč, J., Horvat, M. 2014. In-line NIR monitoring of key characteristics of enteric coated pellets. Eur. J. Pharm. Biopharm. 88, 847–855. http://dx.doi.org/10.1016/j.ejpb.2014.10.003

Mallipeddi, R., Saripella, K. K., Neau, S. H. 2014. Use of fine particle ethylcellulose as the diluent in the production of pellets by extrusion-spheronization. Saudi Pharmaceutical Journal, 22(4), 360–372. https://doi.org/https://doi.org/10.1016/j.jsps.2013.11.001

Pirouz, D. 2006. An Overview of Partial Least Squares. SSRN Electronic Journal. https://dx.doi.org/10.2139/ssrn.1631359

Retsch Technology GmbH. 2007. Operating instruction / Manual Particle Size Analysis System CAMSIZER®.

Tobias, R.D. 1996. An Introduction to Partial Least Squares Regression. [WWW Document]. URL http://support.sas.com/rnd/app/stat/papers/pls.pdf (accessed 27.4.2023)

Vervaet, C., Baert, L., Remon, J. P. 1995. Extrusion-spheronisation A literature review. International Journal of Pharmaceutics, 116(2), 131–146. https://doi.org/10.1016/0378-5173(94)00311-R

TABLES AND FIGURES

Table 1: Optimal response surface experimental design with two numerical and one categorical variable, used to optimize the radial extrusion process. Extrusion screen was set as "hard to change" factor.

Factor / Run order	A: Water quantity [mg/unit]	B: Extrusion speed [RPM]	C: Extrusion screen [mm × mm]
1	75	60	0,5×0,5
2	92,5	15	0,5×0,5
3	110	60	0,5×0,5
4	75	15	0,5×0,5
5	110	15	0,5×0,5
6	92,5	37,5	0,5×0,5
7	92,5	37,5	0,5×0,5
8	92,5	15	0,8×0,7
9	110	15	0,8×0,7
10	92,5	60	0,8×0,7
11	75	37,5	0,8×0,7
12	110	37,5	0,8×0,7
13	75	37,5	0,8×0,7

Table 2: Composition of neutral pellets and film coating dispersion

Material	**Quantity (mg per unit)**
Neutral pellets	
Microcrystalline Cellulose Type 102	95.0 mg
Povidon K30	5.0 mg
Purified Water[1]	75.0 - 110.0 mg
Total neutral pellets:	100.0 mg
Film Coating	
HPMC 6 cP	10.0 mg
Talc	10.0 mg
Tartrazine Sodium	0.15 mg
Purified Water[1]	100.0 mg
Total film coating:	20.15 mg
Total film coated pellets:	120.15 mg

[1] Purified Water evaporates during the process and is not part of the final composition.

Table 3: Top six solutions of numerical optimization with the goal to maximize the process yield and sphericity and minimize the width of particle size distribution (SPAN).

	Factors			**Responses**			**Desirability**
Number	**Water quantity**	**Extrusion speed**	**Extrusion screen**	**Process Yield**	**SPAN**	**Sphericity**	
1	**110,000**	**37,500**	**0,8x0,7**	**89,191**	**0,263**	**0,872**	**0,824**
2	110,000	35,874	0,8x0,7	89,191	0,264	0,872	0,824

3	110,000	41,971	0,8x0,7	89,191	0,262	0,872	0,824
4	110,000	38,255	0,8x0,7	89,191	0,263	0,872	0,824
5	110,000	39,280	0,8x0,7	89,191	0,263	0,872	0,824
6	110,000	44,056	0,8x0,7	89,191	0,263	0,872	0,824

Table 4: Model confirmation showing the predicted value for solution 1 and 95% confidence intervals of prediction. Actual measured values for run 12, performed at the same parameters as proposed by solution 1, fall inside the 95% confidence interval of prediction for all three responses.

Solution 1	**Prediction**			**Run 12 actual values**
Response	**Predicted Mean**	**95% PI low**	**95% PI high**	
Process Yield	89.19%	85.75%	92.63%	87.67%
SPAN	0.263	0.232	0.294	0.275
Sphericity	0.873	0.862	0.882	0.869

Table 5: Predicted values for the first test batch using both NIR probes and UV/VIS determined film coating quantity as a reference. Difference between predicted and reference value shows overprediction of both models.

Test batch 1		**UV/VIS determined film coating quantity**	**Antaris at-line NIR**		**Lighthouse probe in-line NIR**	
Sample No.	**Sampling time**		**Prediction**	**Difference**	**Prediction**	**Difference**
1	11:20	65.1%	70.1%	5%	78.6%	13%
2	11:30	75.9%	79.6%	4%	91.1%	15%
3	11:40	86.3%	92.4%	6%	101.5%	15%
4	11:45	91.4%	95.3%	4%	106.0%	15%
5	11:50 - spraying stopped	96.3%	98.5%	2%	110.9%	15%
6	After drying	101.9%	108.7%	7%	116.9%	15%
				5%		**15%**

Table 6: Predicted values for the second test batch using both NIR probes and UV/VIS determined film coating quantity as a reference. Difference between predicted and reference value shows overprediction of both models.

Test batch 2		**UV/VIS determined film coating quantity**	**Antaris at-line NIR**		**Lighthouse probe in-line NIR**	
Sample No.	**Sampling time**		**Prediction**	**Difference**	**Prediction**	**Difference**
1	12:31	36.9%	38.0%	1%	46.3%	9%
2	12:46	55.4%	59.0%	4%	68.5%	13%
3	13:01	76.2%	80.0%	4%	90.1%	14%
4	13:06	82.7%	86.0%	3%	95.0%	12%
5	13:11	91.3%	93.0%	2%	101.4%	10%
6	13:16	98.3%	100.0%	2%	106.3%	8%
7	13:17 - spraying stopped	97.8%	101.0%	3%	109.0%	11%
8	After drying	100.1%	103.0%	3%	109.8%	10%
				3%		**11%**

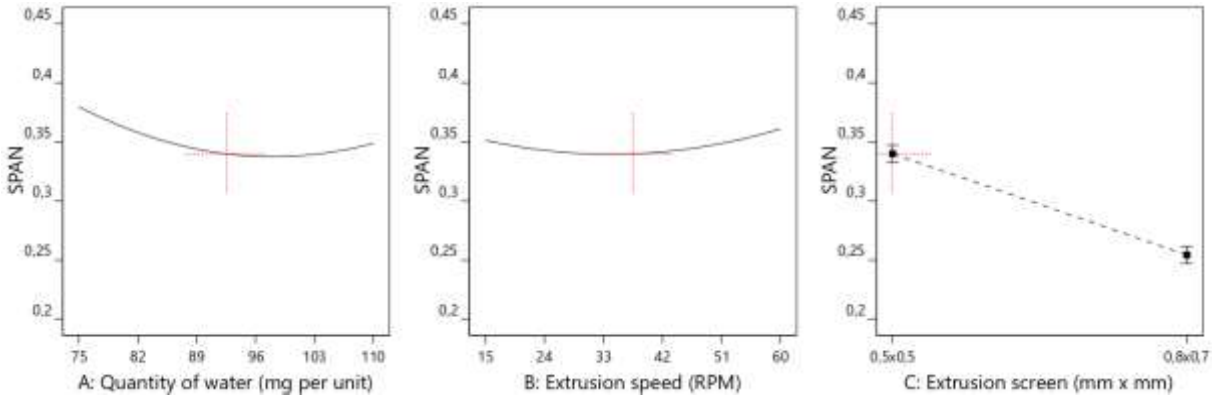

Figure 1: Effects of individual factors on the width of particle size distribution showing the greatest effect comes from the selection of extrusion screen.

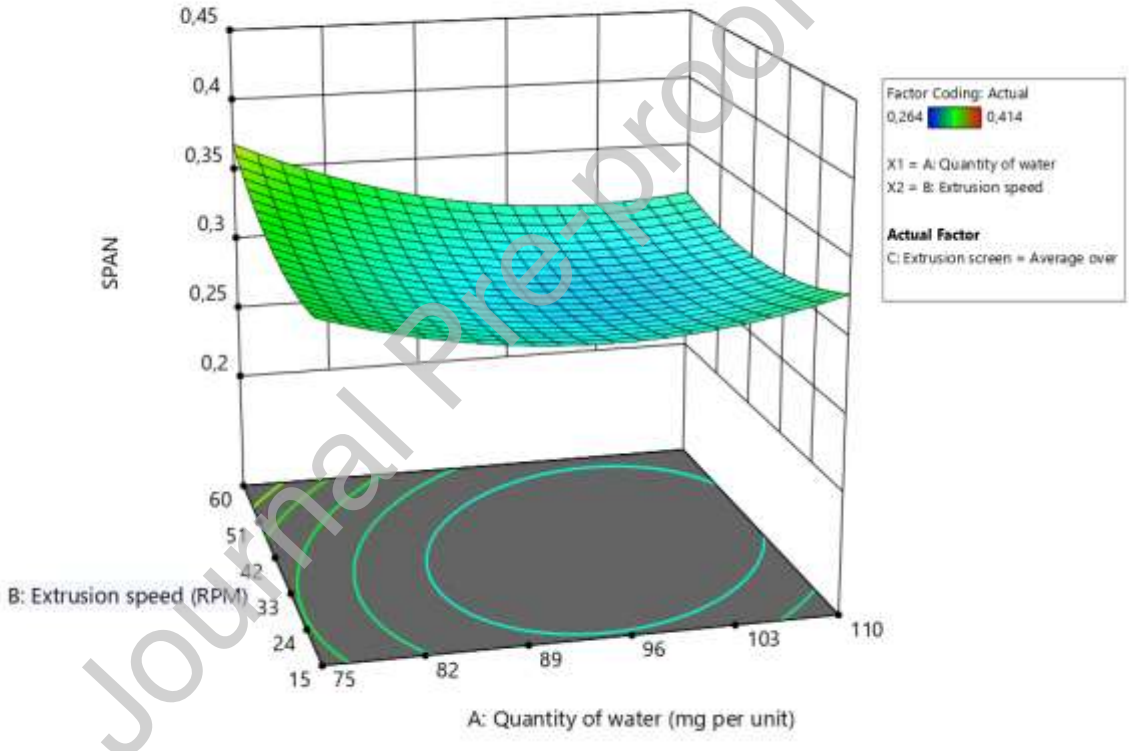

Figure 2: 3D response surface graph showing the interaction between extrusion speed and the quantity of water. Light blue colored area shows the parameters that yield the pellets with the narrowest particle size distribution.

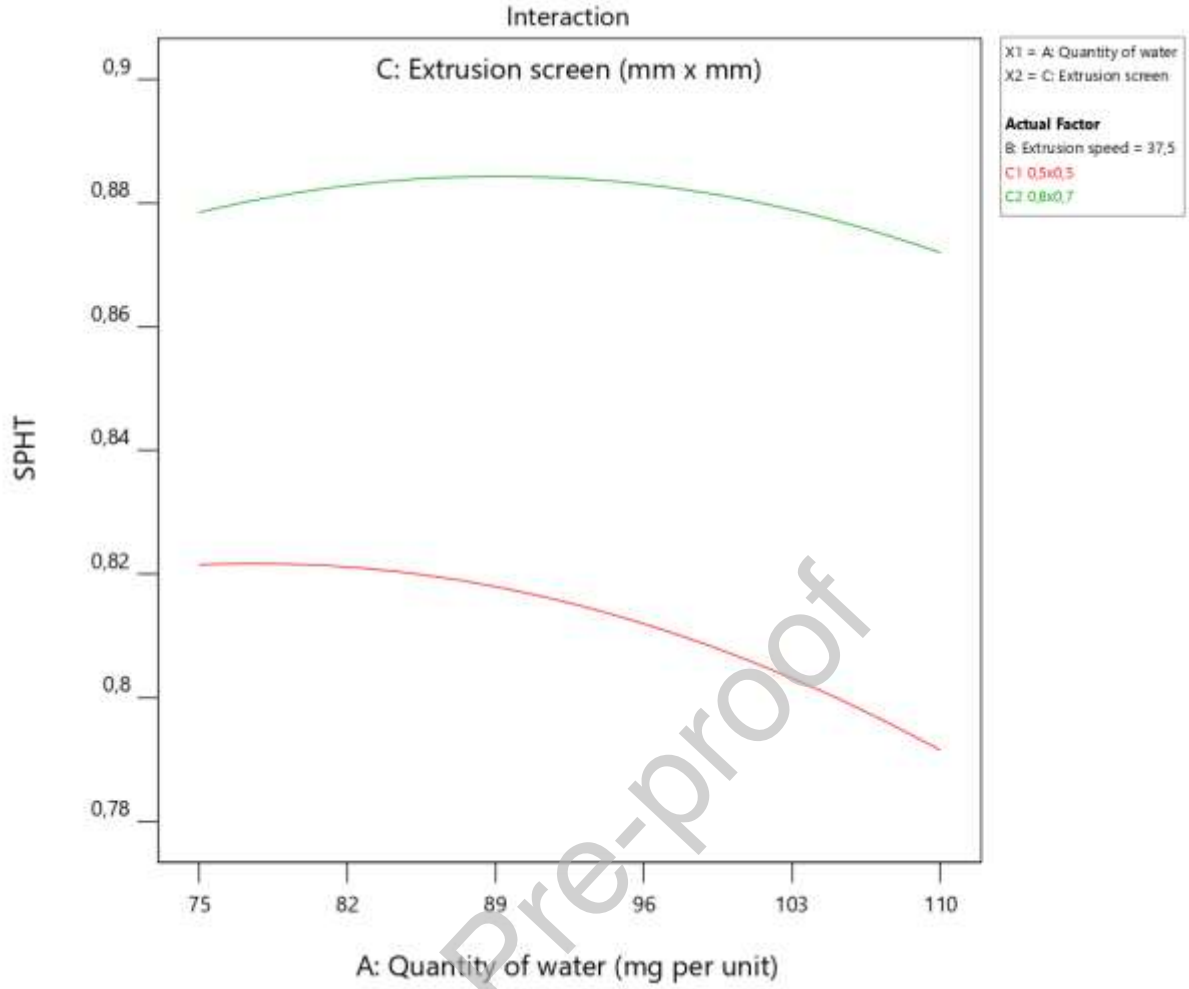

Figure 3: Effect of interaction between the extrusion screen and water quantity on the sphericity (SPHT) of pellets. Use of 0.8 × 0.7 mm extrusion screen produces pellets that are more spherical and the effect of water quantity is less pronounced using that screen. On the other hand, larger water quantity can reduce the sphericity of pellets produced by using the 0.5 × 0.5 mm extrusion screen.

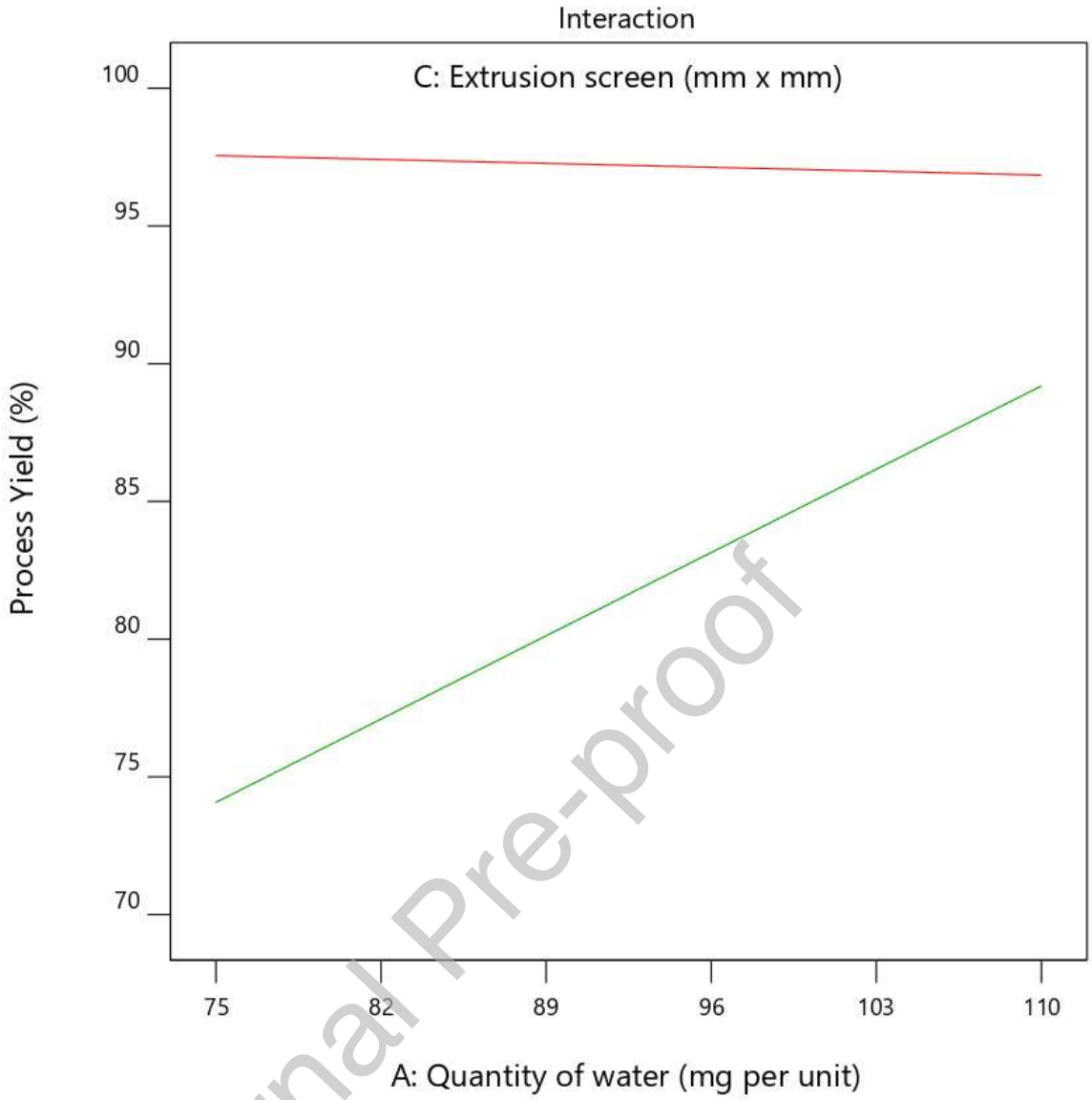

Figure 4: Effect of interaction between the extrusion screen and water quantity on the process yield. Process yield using 0.5 × 0.5 mm screen is significantly higher compared to the 0.8 × 0.7 mm screen and is not significantly affected by water quantity. On the other hand using 0.8 × 0.7 mm screen process yield improves considerably by using higher quantities of water.

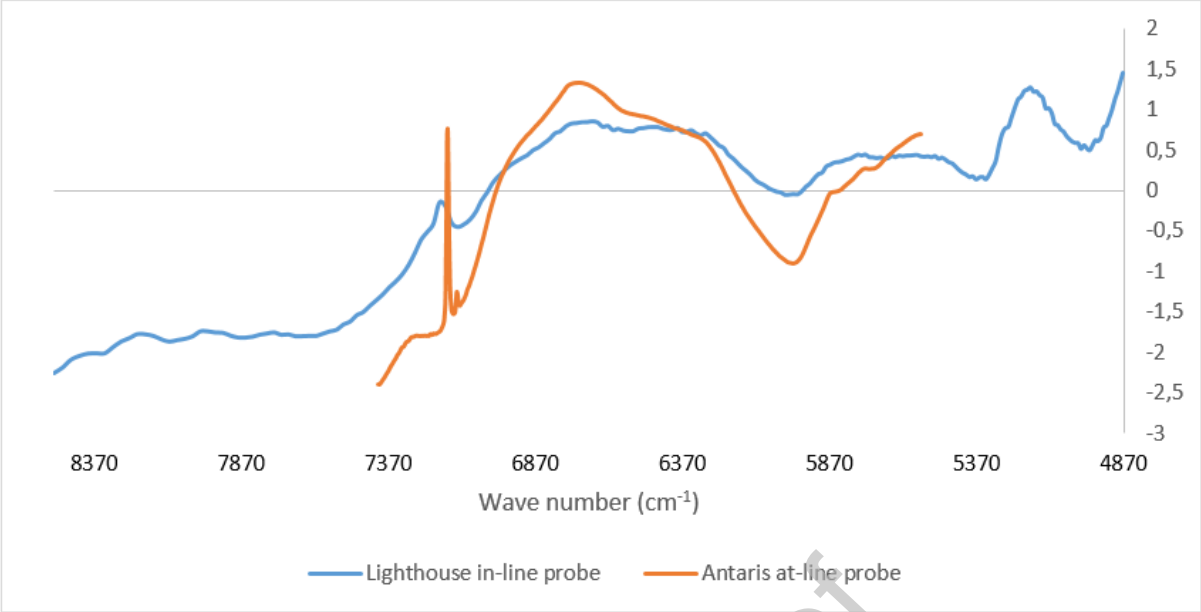

Figure 5: Comparison of SNV transformed NIR spectra of final coated pellets taken by the in-line and the at-line probe. Significant difference in the shape of talc absorption bands at approximately 7150 cm^{-1} can be observed, showing greater resolution of the at-line probe.

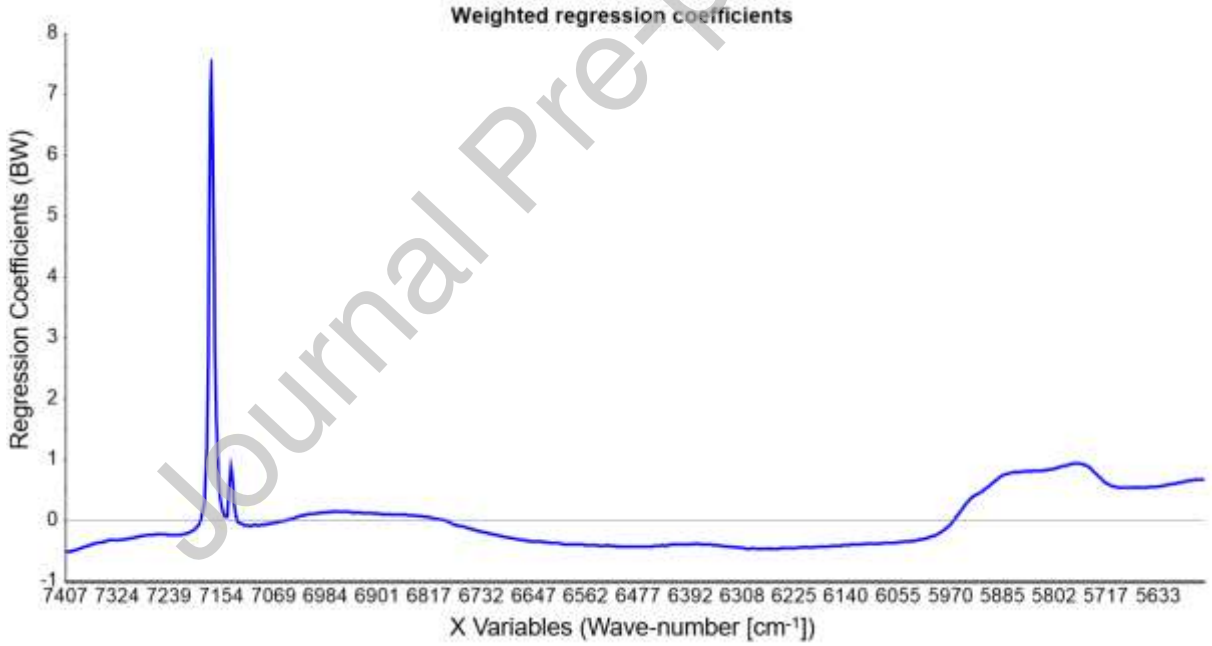

Figure 6: Weighted regression coefficients plot for at-line NIR probe showing the contributions to model variability. Contribution of talc absorption bands (7200 - 7100 cm^{-1}) and HPMC (5900 - 5600 cm^{-1}) can be observed.

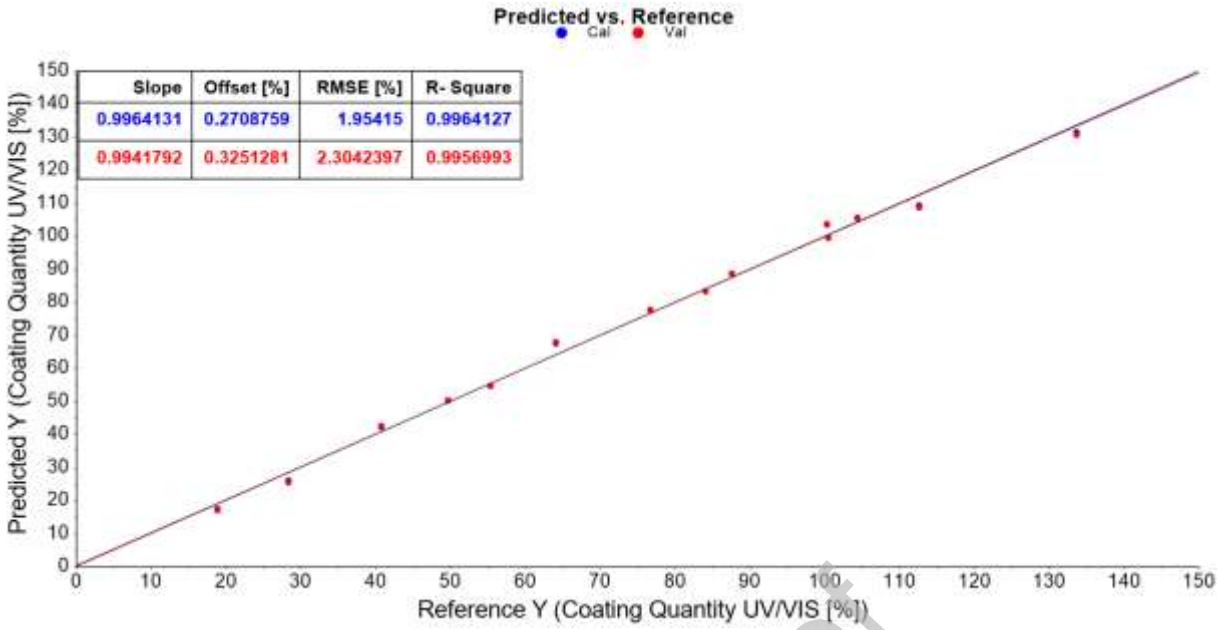

Figure 7: Predicted vs. Reference plot for at-line NIR probe calibration samples. Linear correlation with slope close to 1 and good fit of individual samples can be observed.

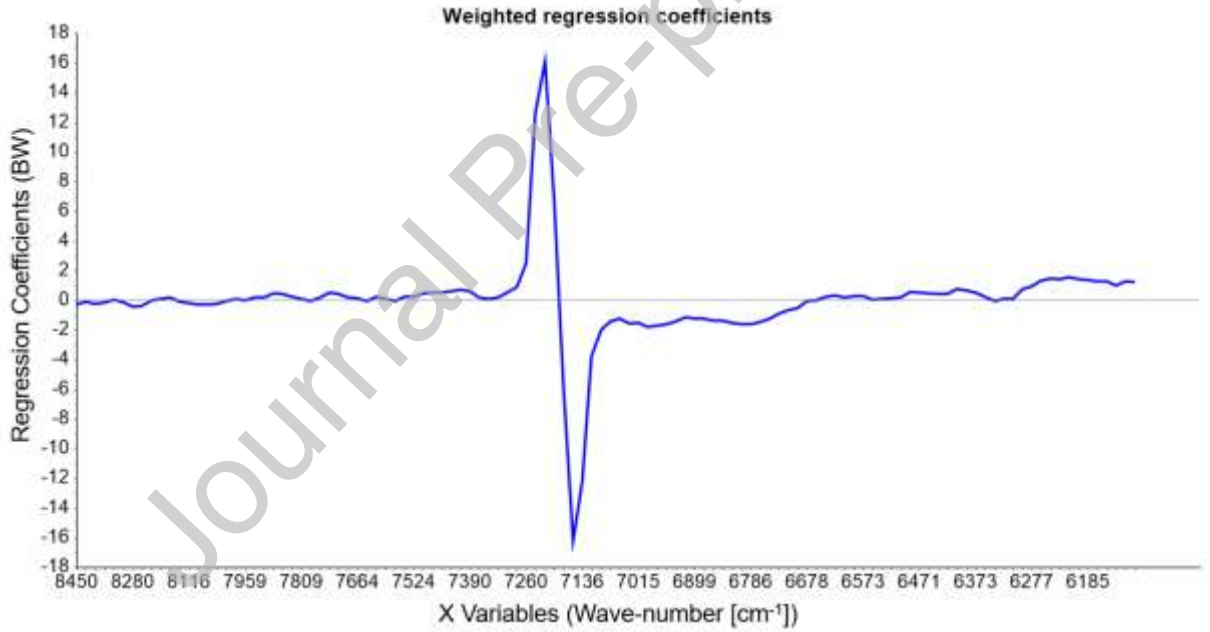

Figure 8: Weighted regression coefficients plot for the in-line NIR probe showing the contributions to model variability. Derived talc absorption band (7220 - 7150 cm^{-1}) contribution and small contribution of water absorption band (6940 cm^{-1}) right next to the talc absorption band can be observed.

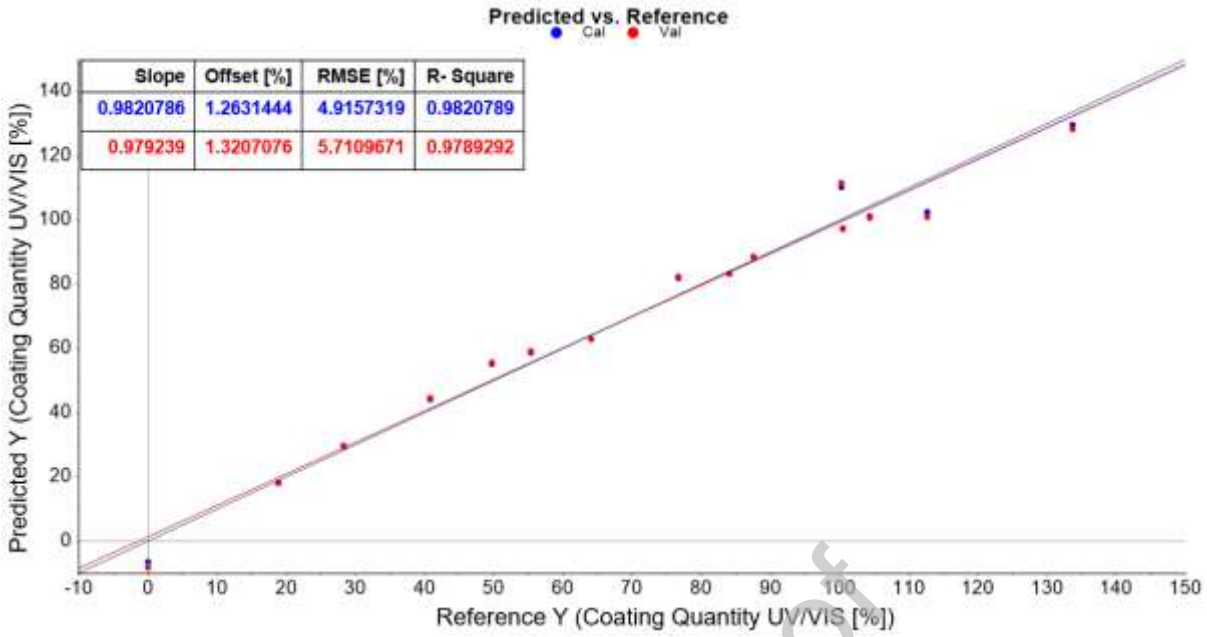

Figure 9: Predicted vs. Reference plot for the in-line NIR probe calibration samples. Linear correlation with slope close to one can be observed. Fit of individual samples is only slightly worse compared to at-line probe.

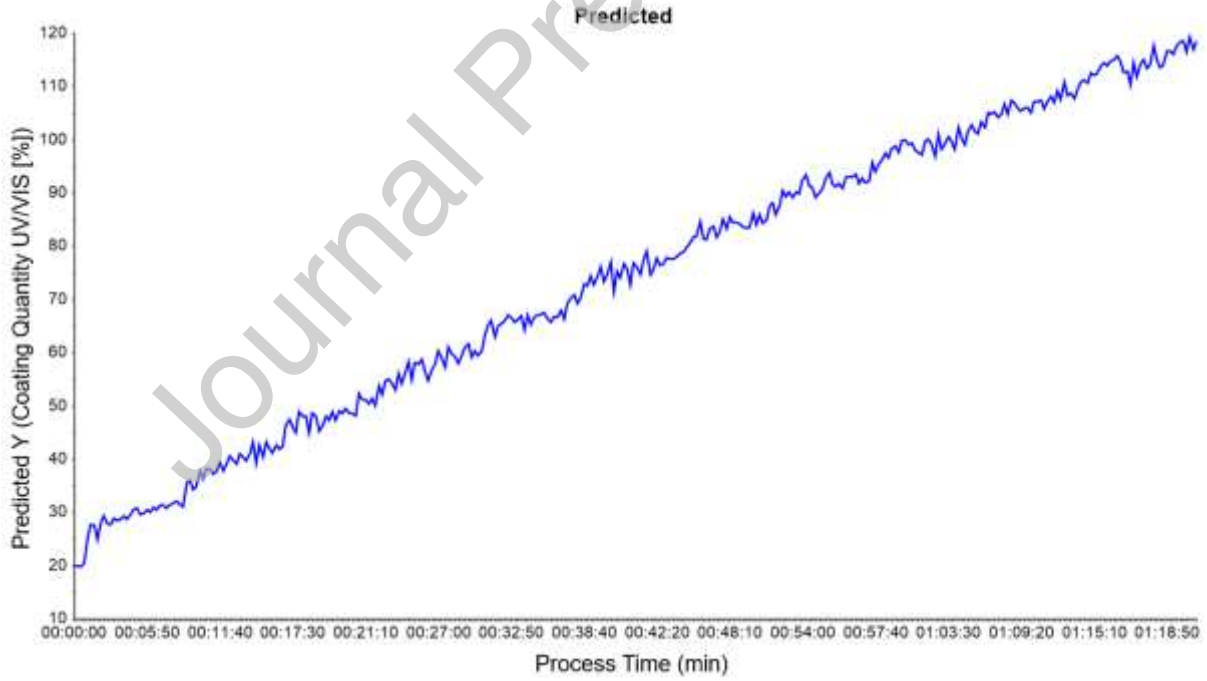

Figure 10: Predicted film coating quantity throughout the coating of the first test batch based on the in-line probe data. Relatively small difference between successive measurements is observed. Model is overpredicting throughout the whole process, with the initial prediction of approximately 20% at the beginning of the spraying process.

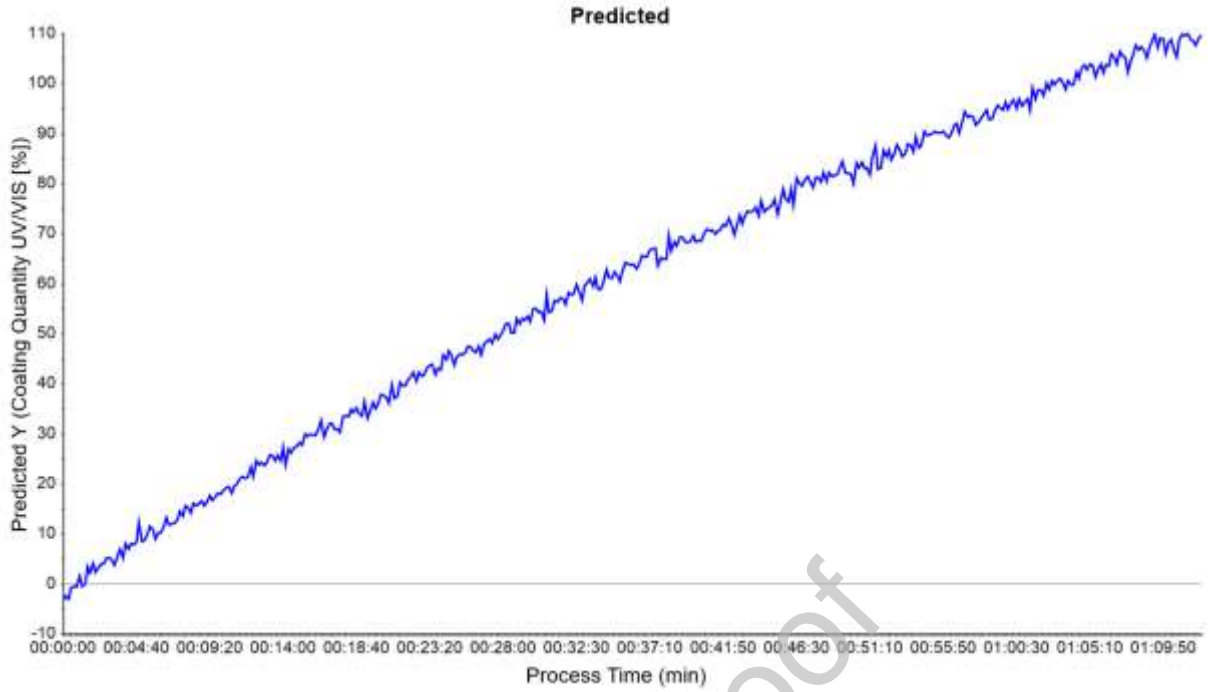

Figure 11: Predicted film coating quantity throughout the coating of the second test batch based on the in-line probe data. Relatively small difference between successive measurements is observed.

Credit author statement

Aljoša Gradišek: Conceptualization, Investigation, Formal analysis, Methodology, Software, Writing - Original Draft

Gregor Ratek: Conceptualization, Supervision, Writing - Review & Editing

Franc Vrečer, PhD: Supervision, Writing - Review & Editing

Klemen Korasa, PhD: Project administration, Conceptualization, Supervision, Writing - Review & Editing

Graphical Abstract